Three generation neutrino oscillation parameters after SNO

Abhijit Bandyopadhyay,* Sandhya Choubey,† Srubabati Goswami,‡ and Kamales Kar§
Saha Institute of Nuclear Physics, 1/AF, Bidhannagar, Kolkata 700 064, India
(Received 10 November 2001; published 3 April 2002)

We examine the solar neutrino problem in the context of the realistic three neutrino mixing scenario including the SNO charged current (CC) rate. The two independent mass squared differences Δm^2_{21} and $\Delta m^2_{31} \approx \Delta m^2_{32}$ are taken to be in the solar and atmospheric ranges, respectively. We incorporate the constraints on Δm^2_{31} as obtained by the SuperKamiokande atmospheric neutrino data and determine the allowed values of Δm^2_{21}, θ_{12} and θ_{13} from a combined analysis of solar and CHOOZ data. Our aim is to probe the changes in the values of the mass and mixing parameters with the inclusion of the SNO data as well as the changes in the two-generation parameter region obtained from the solar neutrino analysis with the inclusion of the third generation. We find that the inclusion of the SNO CC rate in the combined solar+CHOOZ analysis puts a more restrictive bound on θ_{13}. Since the allowed values of θ_{13} are constrained to very small values by the CHOOZ experiment there is no qualitative change over the two generation allowed regions in the $\Delta m^2_{21} - \tan^2\theta_{12}$ plane. The best fit comes in the LMA region and no allowed area is obtained in the SMA region at the 3σ level from combined solar and CHOOZ analysis.

DOI: 10.1103/PhysRevD.65.073031 PACS number(s): 14.60.Pq, 12.15.Ff, 26.65.+t

I. INTRODUCTION

The recent results on charged current measurement from Sudbury Neutrino Observatory (SNO) [1] have confirmed the solar neutrino shortfall as observed in the earlier experiments [2–5]. A comparison of the SuperKamiokande and SNO results establishes the presence of a nonelectron flavor component in the solar neutrino flux received at Earth (at more than 3σ level) in a model independent manner [1,6–8]. Neutrino oscillation provides the most popular explanation of this anomaly. A two generation analysis of the solar neutrino data including the SNO results has been performed by various groups [7,9–15]. All these analyses agree that the best description of the data on the total rates and the day-night spectrum data of the SuperKamiokande (SK) Collaboration is provided by the large mixing angle (LMA) Mikheyev-Smirnov-Wolfenstein (MSW) solution ($\Delta m^2_\odot \sim 10^{-5}$ eV^2), though the low $\Delta m^2_\odot$ solution [(LOW) quasi vacuum oscillation (QVO)] ($\Delta m^2_\odot \sim 10^{-9} - 10^{-7}$ eV^2) and the vacuum oscillation (VO) solutions ($\Delta m^2 \sim 4.5 \times 10^{-10}$ eV^2) are also allowed. The small mixing angle (SMA) MSW solution is largely disfavored with no allowed contour in the mass-mixing plane at the 3σ level.[1] On the other hand, for the explanation of the atmospheric neutrino anomaly the two generation oscillation analysis of the atmospheric neutrino data requires $\Delta m^2_{atm} \sim 10^{-3}$ eV^2 [16]. Since the allowed ranges of $\Delta m^2_\odot$ and Δm^2_{atm} are completely nonoverlapping, to explain the solar and atmospheric neutrino data simultaneously by neutrino oscillation one requires at least two independent mass-squared differences and consequently three active neutrino flavors which fits very nicely with the fact that to date we have observed three neutrino flavors in nature. Thus to get the complete picture of neutrino masses and mixing a three generation analysis is called for. Apart from the solar and atmospheric neutrinos positive evidence for neutrino oscillation is also published by the Liquid Scintillator Neutrino Detector (LSND) experiment [17] and although there had been several attempts to explain all the three sources of evidence in a three generation picture it is now widely believed that to accommodate the LSND results one has to introduce an additional sterile neutrino [18,19]. For the purpose of this analysis we ignore the LSND results. We incorporate the negative results from the CHOOZ reactor experiment on the measurement of $\overline{\nu}_e$ oscillation by the disappearance technique [20]. CHOOZ is sensitive to $\Delta m^2_{CHOOZ} \gtrsim 10^{-3}$ eV^2 which is the range probed in the atmospheric neutrino measurements and together they can put important constraints on the three neutrino mixing parameters. We consider the three flavor picture with

$$\Delta m^2_{21} = \Delta m^2_\odot ,$$

$$\Delta m^2_{31} = \Delta m^2_{CHOOZ} \simeq \Delta m^2_{atm} = \Delta m^2_{32} .$$

Three flavor oscillation analysis of solar, atmospheric and CHOOZ data assuming this mass spectrum was performed in the pre-SNO era by different groups [21–23]. We investigate

*Email address: abhi@theory.saha.ernet.in
†Email address: sandhya@theory.saha.ernet.in
‡Email address: sruba@theory.saha.ernet.in
§Email address: kamales@theory.saha.ernet.in

[1]The only exception is the analysis of [9] which gets a small allowed region for the SMA solution due to a slight difference in the treatment of the data.

 ©2002 The American Physical Society

the impact of the charged current measurement at SNO on neutrino mass and mixing in a three flavor scenario and present the most up to date status of the allowed values of three flavor oscillation parameters.

The plan of the paper is as follows. In Sec. II we present the relevant probabilities. In Sec. III we discuss the χ^2-analysis method and the results. We end in Sec. IV with some discussion and conclusions.

II. CALCULATION OF PROBABILITIES

The three-generation mixing matrix that we use is

$$U = R_{23}R_{13}R_{12} = \begin{pmatrix} c_{13}c_{12} & s_{12}c_{13} & s_{13} \\ -s_{12}c_{23}-s_{23}s_{13}c_{12} & c_{23}c_{12}-s_{23}s_{13}s_{12} & s_{23}c_{13} \\ s_{23}s_{12}-s_{13}c_{23}c_{12} & -s_{23}c_{12}-s_{13}s_{12}c_{23} & c_{23}c_{13} \end{pmatrix}, \quad (1)$$

where we neglect the CP violation phases. This is justified as one can show that the survival probabilities P_{ee} of the electron neutrinos do not depend on these phases. The above choice has the advantage that the matrix elements U_{e1}, U_{e2} and U_{e3} relevant for the solar neutrino problem become independent of θ_{23} while the elements U_{e3}, $U_{\mu 3}$ and $U_{\tau 3}$ relevant for the atmospheric neutrino problem are independent of θ_{12}. The mixing angle common to both solar and atmospheric neutrino sectors is θ_{13} which, as we will see, is constrained severely by the CHOOZ data.

A. Solar neutrinos

The general expression for the survival amplitude for an electron neutrino arriving on the Earth from the Sun, in the presence of three neutrino flavors, is given by [24]

$$A_{ee} = A^{\odot}_{e1}A^{vac}_{11}A^{\oplus}_{1e} + A^{\odot}_{e2}A^{vac}_{22}A^{\oplus}_{2e} + A^{\odot}_{e3}A^{vac}_{33}A^{\oplus}_{3e}, \quad (2)$$

where $A^{\odot}_{ek}$ gives the probability amplitude of $\nu_e \to \nu_k$ transition at the solar surface, A^{vac}_{kk} gives the transition amplitude from the solar surface to the Earth surface, and $A^{\oplus}_{ke}$ denotes the $\nu_k \to \nu_e$ transition amplitudes inside the Earth. One can write the transition amplitudes in the Sun as an amplitude part times a phase part

$$A^{\odot}_{ek} = a^{\odot}_{ek} e^{-i\phi^{\odot}_k}. \quad (3)$$

$a^{\odot 2}_{ek}$ can be expressed as

$$a^{\odot 2}_{ek} = \sum_{j=1,2,3} X_{kj} U^{\odot 2}_{je}, \quad (4)$$

where X_{kj} denotes the nonadiabatic jump probability between the jth and kth state and $U^{\odot}_{je}$ denotes the mixing matrix element between the flavor state ν_e and the mass state ν_j in the Sun. A^{vac}_{kk} is given by

$$A^{vac}_{kk} = e^{-iE_k(L-R_{\odot})}, \quad (5)$$

where E_k is the energy of the state ν_k, L is the distance between the center of the Sun and Earth and $R_{\odot}$ is the solar radius. For a two slab model of the Earth, a mantle and core with constant densities of 4.5 and 11.5 g/cm^{-3} respectively, the expression for $A^{\oplus}_{ke}$ can be written as (assuming the flavor states to be continuous across the boundaries) [25]

$$A^{\oplus}_{ke} = \sum_{\substack{i,j,l, \\ \alpha,\beta,\sigma}} U^M_{el} e^{-i\psi^M_l} U^M_{\alpha l} U^C_{\alpha i} e^{-i\psi^C_i} U^C_{\beta i} U^M_{\beta j} e^{-i\psi^M_j} \times U^M_{\sigma j} U_{\sigma k}, \quad (6)$$

where (i,j,l) denotes mass eigenstates and (α,β,σ) denotes flavor eigenstates, U^M and U^C are the mixing matrices in the mantle and the core respectively and ψ^M and ψ^C are the corresponding phases picked up by the neutrinos as they travel in the mantle and the core of the Earth:

$$P_{ee} = |A_{ee}|^2 = \Sigma_k a^{\odot}_{ei} |A^{\oplus}_{ke}|^2 + \sum_{l>k} 2 a^{\odot}_{ek} a^{\odot}_{el} Re[A^{\oplus}_{ke} A^{\oplus}_{le} \times e^{i(E_l - E_k)(L-R_{\odot})} e^{i(\phi^{\odot}_l - \phi^{\odot}_k)}]. \quad (7)$$

This is the most general expression for the probability [26]. Since for our case $\Delta_{31} \approx \Delta_{32}$ is $\sim 10^{-3}$ eV^2 the phase terms $e^{i(E_3-E_1)(L-R_{\odot})}$ and $e^{i(E_3-E_2)(L-R_{\odot})}$ average out to zero. Therefore the probability simplifies to

$$P_{ee} = a^{\odot 2}_{e1} |A^{\oplus}_{1e}|^2 + a^{\odot 2}_{e2} |A^{\oplus}_{2e}|^2 + a^{\odot 2}_{e3} |A^{\oplus}_{3e}|^2 + 2 a^{\odot}_{e1} a^{\odot}_{e2} Re[A^{\oplus}_{1e} A^{\oplus *}_{2e} \times e^{i(E_2-E_1)(L-R_{\odot})} e^{i(\phi^{\odot}_2 - \phi^{\odot}_1)}]. \quad (8)$$

The mixing matrix elements in matter are different from those in vacuum and it is in general a difficult task to find the matter mixing angles and eigenvalues for a 3×3 matrix. However in our case since $\Delta m^2_{31} \gg \Delta m^2_{21} \approx$ the matter potential in the Sun, the ν_3 state experiences almost no matter effect and MSW resonance can occur between ν_2 and ν_1

states. Under this approximation the three generation survival probability for the electron neutrino can be expressed as

$$P_{ee}=c_{13}^4 P_{ee}^{2gen}+s_{13}^4, \tag{9}$$

where P_{ee}^{2gen} is of the two generation form in the mixing angle θ_{12}:

$$P_{ee}^{2gen}=P_{ee}^{day}+\frac{(2P_{ee}^{day}-1)(\sin^2\theta_{12}-|A_{2e}^{\oplus}|^2)}{\cos 2\theta_{12}}, \tag{10}$$

where

$$P_{ee}^{day}=0.5+[0.5-\Theta(E-E_A)X_{12}]\cos 2\theta_{12}^{\odot}\cos 2\theta_{12}, \tag{11}$$

with

$$\tan 2\theta_{12}^{\odot}=\frac{\Delta m_{21}^2 \sin 2\theta_{12}}{\Delta m_{21}^2\cos 2\theta_{12}-Ac_{13}^2}, \tag{12}$$

where A denotes the matter potential,

$$A=2\sqrt{2}G_F n_e^{\odot}E. \tag{13}$$

Here $n_e^{\odot}$ is the electron density in the Sun, E the neutrino energy, and $\Delta m_{21}^2(=m_2^2-m_1^2)$ the mass squared difference in vacuum. The jump probability X_{12} continues to be given by the two-generation expression and for this we use the analytic expression given in [27]. E_A in the Heaviside function Θ gives the minimum ν_e energy that can encounter a resonance inside the Sun and is given by

$$E_A=\Delta m_{21}^2\cos 2\theta_{12}/2\sqrt{2}G_F n_e|_{pr}, \tag{14}$$

$n_e|_{pr}$ being the electron density at the point of production. In the limit $\theta_{13}=0$ one recovers the two generation limit.

B. The probability for CHOOZ

The survival probability relevant for the CHOOZ experiment for the three generation case is

$$P_{ee}=1-c_{13}^4\left[\sin^2 2\theta_{12}\sin^2\frac{\Delta m_{21}^2 L}{4E}\right]-\sin^2 2\theta_{13}\sin^2\frac{\Delta m_{31}^2 L}{4E}+\sin^2 2\theta_{13}s_{12}^2\left[\sin^2\frac{\Delta m_{31}^2 L}{4E}-\sin^2\frac{(\Delta m_{31}^2-\Delta m_{21}^2)L}{4E}\right]. \tag{15}$$

Since the average energy of the neutrinos in the CHOOZ experiment is ~ 1 MeV and the distance traveled by the neutrinos is of the order of 1 km the $\sin^2(\Delta m_{21}^2 L/4E)$ term is important only for $\Delta m_{21}^2 \gtrsim 3\times 10^{-4}$ eV^2. The last term in the above expression is an interference term between both mass scales [28] and is absent if one uses the approximation $\Delta_{31}=\Delta_{32}$ and is often ignored.

TABLE I. The ratio of the observed solar neutrino rates to the corresponding BBP00 SSM predictions.

Experiment	$\frac{observed}{BBP00}$	Composition
Cl	0.335 ± 0.029	$B(75\%), Be(15\%)$
Ga	0.584 ± 0.039	$pp(55\%), Be(25\%), B(10\%)$
SK	0.459 ± 0.017	$B(100\%)$
SNO(CC)	0.347 ± 0.027	$B(100\%)$

III. THE χ^2 ANALYSIS

The definition of $\chi_{\odot}^2$ used in our fits is

$$\chi_{\odot}^2=\sum_{i,j=1,4}(R_i^{\rm th}-R_i^{\rm exp})[(\sigma_{ij}^{rates})^2]^{-1}(R_j^{\rm th}-R_j^{\rm exp}) + \sum_{i,j=1.38}(X_n S_i^{\rm th}-S_i^{\rm exp})[(\sigma_{ij}^{spm})^2]^{-1} \times (X_n S_j^{\rm th}-S_j^{\rm exp}), \tag{16}$$

where R_i^{ξ} ($\xi=$th or exp) denote the total rate while S_i^{ξ} denote the SK spectrum in the ith bin. Both the experimental and theoretical values of the fitted quantities are normalized relative to the Bahcall-Basu-Pinsonneault 2000 (BBP00) [29] predictions. The experimental values for the total rates are the ones shown in Table I, while the SK day-night spectra are taken from [2]. The error matrix $(\sigma^{rates})^2$ contains the experimental errors, the theoretical errors (which includes error in the capture cross sections and the astrophysical uncertainties in BBP00 predictions) along with their correlations. It is evaluated using the procedure of [30]. The error matrix for the spectrum $(\sigma^{spm})^2$ contains the correlated and uncorrelated errors as discussed in [31]. The details of the solar code used is described in [10,32,12,14]. We vary the normalization of the SK spectrum X_n as a free parameter to avoid double counting with the SK data on the total rate. Thus there are $(38-1)$ independent data points from the SK day-night spectrum along with the 4 total rates giving a total of 41 data points. For the analysis of only the solar data in the three-generation scheme, we have $(41-3)$ degrees of freedom (DOF). The best-fit values of parameters and the χ_{min}^2 are

$$\Delta m_{21}^2=4.7\times 10^{-5}\ \text{eV}^2,\quad \tan^2\theta_{12}=0.375,$$

$$\tan^2\theta_{13}=0.0,\quad \chi_{min}^2=33.42.$$

Hence the best-fit comes in the two-generation limit presented in [10,12,14].

We next incorporate the results from the CHOOZ reactor experiment [20]. The definition of χ_{CHOOZ}^2 is given by [33]

$$\chi_{CHOOZ}^2=\sum_{j=1,15}\left(\frac{x_j-y_j}{\Delta x_j}\right)^2, \tag{17}$$

where x_j are the experimental values, y_j are the corresponding theoretical predictions, Δx_j are the 1σ errors in the ex-

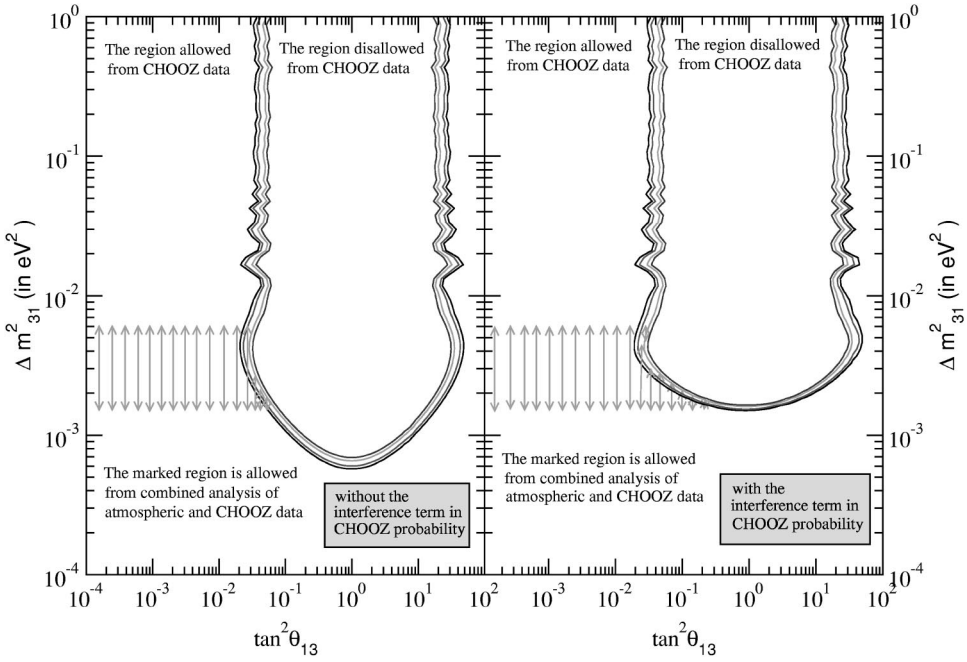

FIG. 1. The allowed areas in $(\tan^2\theta_{13}-\Delta m^2_{31})$ plane from atmospheric and CHOOZ data.

perimental quantities and the sum is over 15 energy bins of data of the CHOOZ experiment [20]. The global χ^2 for solar +CHOOZ analysis is defined as

$$\chi^2_{global}=\chi^2_{\odot}+\chi^2_{CHOOZ}. \tag{18}$$

The total number of data points for combined solar and CHOOZ analysis is therefore $41+15=56$. The solar +CHOOZ analysis depends on Δm^2_{21}, Δm^2_{31}, θ_{12} and θ_{13}. For unconstrained Δm^2_{31}, the χ^2_{min} and the best-fit values are

$$\Delta m^2_{21}=4.7\times10^{-5}\ \text{eV}^2,\quad \tan^2\theta_{12}=0.374,$$

$$\Delta m^2_{31}=1.35\times10^{-3}\ \text{eV}^2,\quad \tan^2\theta_{13}=1.74\times10^{-3},$$

$$\chi^2_{min}=39.75.$$

However the atmospheric neutrino data imposes strong constraints on the allowed range of Δm^2_{31}. The combined analysis of the 1289 day atmospheric data and the CHOOZ data restricts allowed Δm^2_{31} in the range $[1.5,6]\times10^{-3}$ eV^2 at 99% C.L. [21]. Thus the best fit $\Delta m^2_{31}=1.35\times10^{-3}$ that we obtain from the solar+CHOOZ analysis falls outside the allowed range. If we restrict the range of Δm^2_{31} from the combined analysis of the atmospheric+CHOOZ analysis [21] then the χ^2_{min} and the best-fit parameters obtained from the combined solar+CHOOZ analysis are

$$\Delta m^2_{21}=4.7\times10^{-5}\ \text{eV}^2,\quad \tan^2\theta_{12}=0.374,$$

$$\Delta m^2_{31}=1.5\times10^{-3}\ \text{eV}^2,\quad \tan^2\theta_{13}=1.46\times10^{-3},$$

$$\chi^2_{min}=39.75.$$

Thus the best fit for the solar+CHOOZ analysis comes almost at the two generation limit, with the best fit Δm^2_{31} at the lower limit of the allowed range. For 52 DOF this solution is allowed at 89.33%. The improvement in the goodness of fit (GOF) in comparison to the two flavor analysis presented in [10,12,14] is due to the inclusion of the CHOOZ data which gives a χ^2/DOF of about 6/15.

IV. ALLOWED AREAS IN THE THREE GENERATION PARAMETER SPACE

A. Constraints on the $\Delta m^2_{31}-\tan^2\theta_{13}$ plane

For the chosen mass spectrum and mixing matrix the relevant survival probabilities for atmospheric neutrinos depend on the parameters θ_{23}, θ_{13} and $\Delta m^2_{32}(\simeq\Delta m^2_{31})$ [22] while the CHOOZ survival probability $P_{\overline{ee}}$ depends mainly on θ_{13} and Δm^2_{31} and very mildly on θ_{12} and Δm^2_{21}. In Fig. 1 we plot the allowed domains in the $\tan^2\theta_{13}-\Delta m^2_{31}$ parameter space from the analysis of only the CHOOZ data keeping all other parameters free. We give this plot both with and without taking into account the interference term. The effect of the interference term is to lift the allowed ranges of Δm^2_{31}. The shaded area marked by arrows in this figure is the allowed range from a combined analysis of 1289 day atmospheric data and CHOOZ data taken from [21]. At 99% C.L. the atmospheric+CHOOZ analysis allows $\tan^2\theta_{13}\lesssim0.08$ and 1.5×10^{-3} eV^2 $<\Delta m^2_{31}<6.0\times10^{-3}$ eV^2. It also becomes apparent from this figure that for $\tan^2\theta_{13}\lesssim0.03$, all values of Δm^2_{31} in the range $[1.5,6.0]\times10^{-3}$ eV^2 are allowed at 99% C.L. whereas for $0.03\lesssim\tan^2\theta_{13}\lesssim0.075$, certain values of Δm^2_{13} get excluded. A closer inspection of Fig. 1 shows that around $\tan^2\theta_{13}\sim0.03$ a window in Δm^2_{31} is disallowed whereas for higher values of $\tan^2\theta_{13}$ certain regions of Δm^2_{13} towards higher values of the interval $[1.5,6.0]\times10^{-3}$ eV^2 get disallowed. The width of the disallowed range in Δm^2_{31} depends on $\tan^2\theta_{13}$. Clearly the Δm^2_{31} is restricted more from the atmospheric data while the more stringent bound on $\tan^2\theta_{13}$ comes from the CHOOZ results. It is also evident

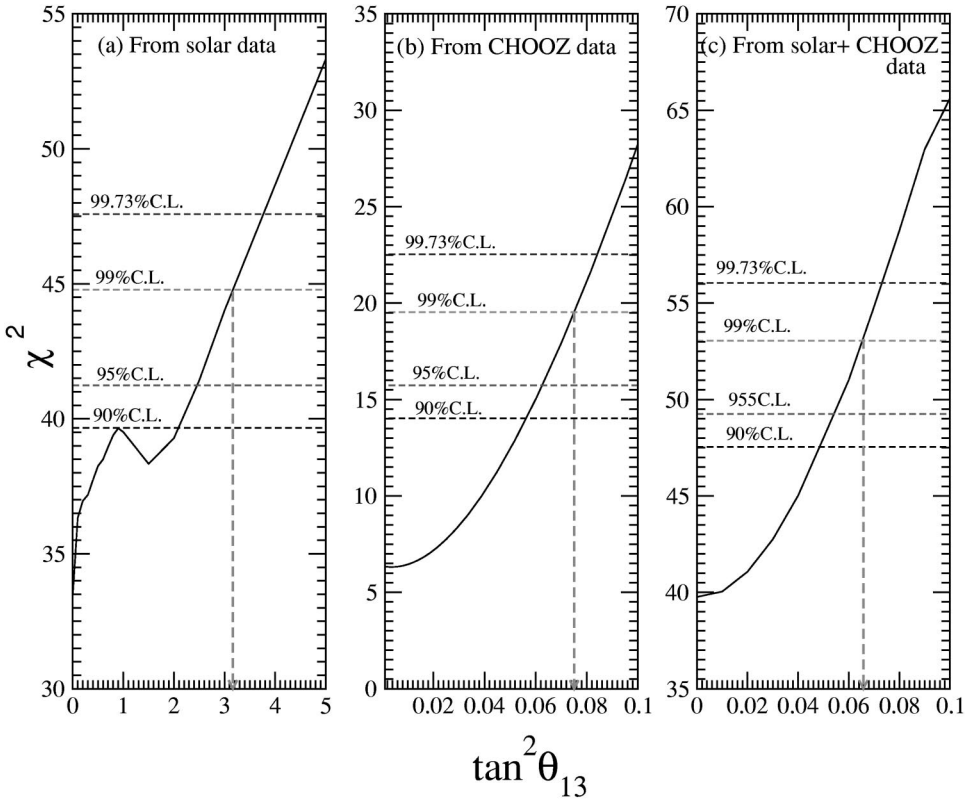

FIG. 2. The plot of χ^2 vs $\tan^2\theta_{13}$ from (a) solar, (b) CHOOZ, and (c) solar+CHOOZ data.

that the region in Δm^2_{31} which is disallowed in the only CHOOZ contour once the interference effects are taken into account is also being disallowed by the combined atmospheric and CHOOZ analysis. In Figs. 2(a), 2(b), and 2(c) we plot the $\chi^2_{\odot}$, χ^2_{CHOOZ}, and $\chi^2_{\odot}+\chi^2_{CHOOZ}$ respectively against $\tan^2\theta_{13}$, keeping θ_{12}, Δm^2_{21} and Δm^2_{31} (in the range $[1.5,6.0]\times 10^{-3}$ eV^2) free. It is clear from the three figures that the most stringent bound on $\tan^2\theta_{13}(<0.065$ at 99% C.L.) comes from the combined solar and CHOOZ analysis. The pre-SNO bound on $\tan^2\theta_{13}$ that we get from the combined solar+CHOOZ analysis is $\tan^2\theta_{13}\lesssim 0.075$. Thus SNO is seen to tighten the constraint on the θ_{13} mixing angle such that the most stringent upper limit on θ_{13} is obtained from the solar plus CHOOZ analysis.

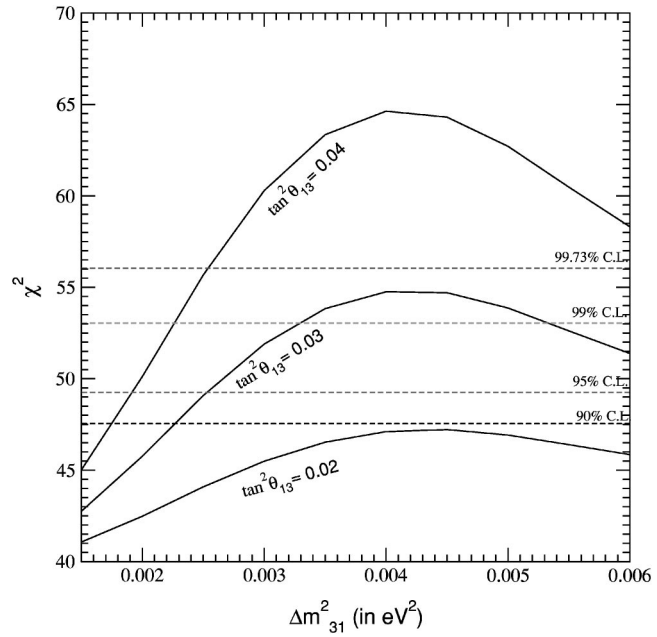

FIG. 3. The plot of χ^2 vs Δm^2_{31} from solar+CHOOZ data.

B. Probing the $\Delta m^2_{21}-\tan^2\theta_{12}$ parameter space

We now attempt to explore the 1–2 parameter space from a combined solar+CHOOZ analysis, in the light of new results from SNO. The parameters θ_{12} and Δm^2_{21} are mainly constrained from the solar data. We present in Fig. 3 the allowed areas in the 1–2 plane at 90%, 95%, 99% and 99.73% confidence levels for different sets of the combination of Δm^2_{31} and $\tan^2\theta_{13}$, lying within their respective allowed range from atmospheric+CHOOZ and solar +CHOOZ analysis. The CHOOZ data limits the upper allowed range of Δm^2_{12} in the LMA region to 3×10^{-4} eV^2. In the three flavor scenario also there is no room for SMA MSW solution at the 3σ level (99.73% C.L.).[2] We see from Fig. 3 that the allowed regions reduce in size as we increase $\tan^2\theta_{13}$ for a fixed Δm^2_{31}. At the upper limit of the allowed range of Δm^2_{31} the LOW solution gets completely disallowed

[2]We find that for values of $\tan^2\theta_{13}>0.25$, one gets allowed areas in the SMA region at 3σ level even after including the SNO data. Beyond this value of $\tan^2\theta_{13}$ the allowed area in the SMA region increases and finally for larger values of $\tan^2\theta_{13}$ the SMA and LMA regions merge with each other. However, these large values of $\tan^2\theta_{13}$ lie outside the range allowed by CHOOZ.

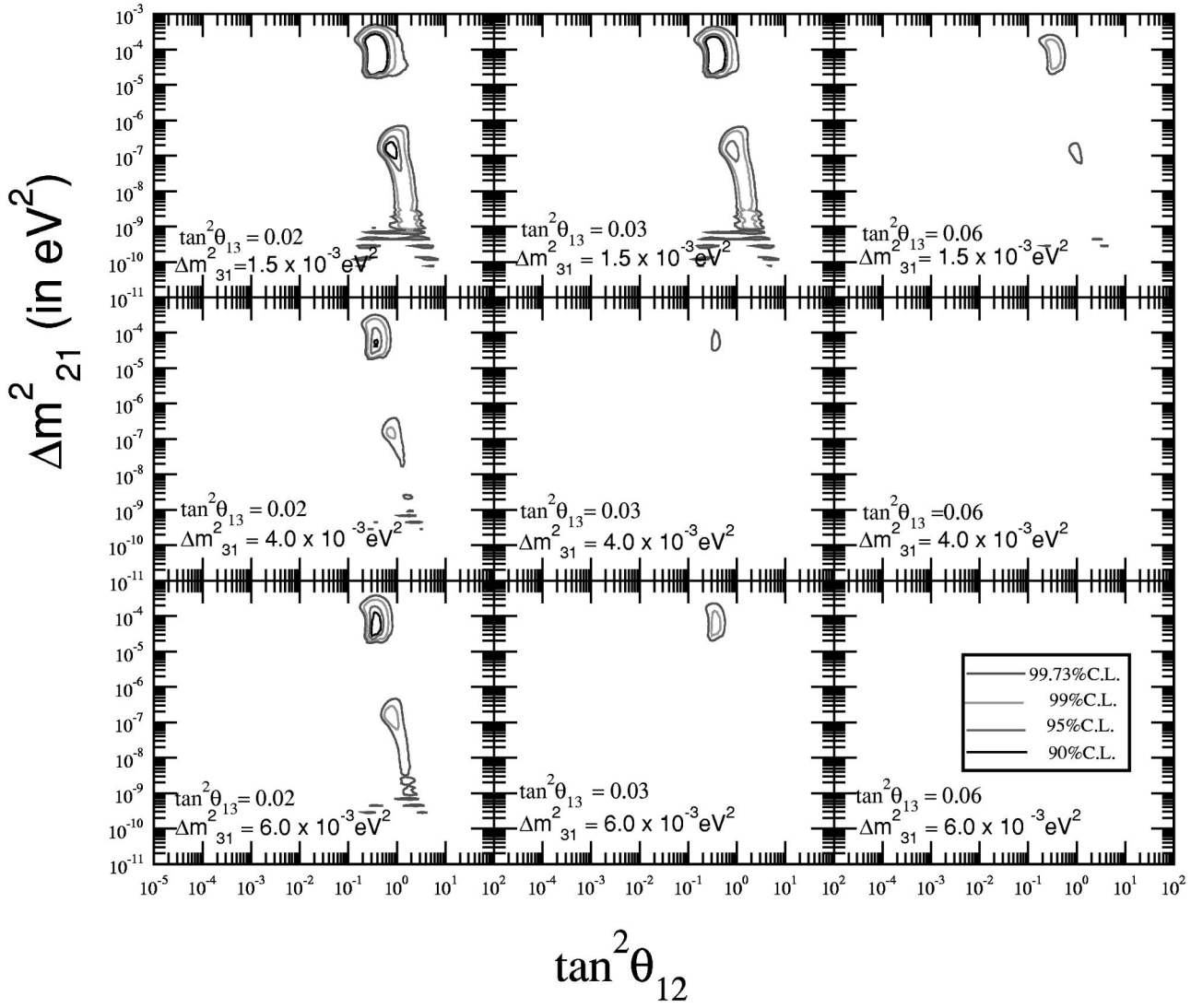

FIG. 4. The allowed areas in ($\tan^2\theta_{12} - \Delta m^2_{21}$) plane from solar+CHOOZ analysis.

beyond $\tan^2\theta_{13} \sim 0.02$ while the LMA solution gets disallowed beyond $\tan^2\theta_{13} \sim 0.03$. At the lower limit of of Δm^2_{31} the LMA solution is found to disappear at 99% C.L. beyond $\tan^2\theta_{13} \sim 0.065$, which is the upper bound of $\tan^2\theta_{13}$ at 99% C.L., obtained from solar+CHOOZ analysis. On the other hand, for any given $\tan^2\theta_{13}$ the least allowed area in $\tan^2\theta_{12} - \Delta m^2_{21}$ parameter space occurs at $\Delta m^2_{31} \sim 4.0 \times 10^{-3}$ eV^2, whereas above and below this value larger regions of parameter space are allowed. To illustrate this in Fig. 4 we plot the $\chi^2_\odot + \chi^2_{CHOOZ}$ vs Δm^2_{31} for fixed $\tan^2\theta_{13}$ allowing the other parameters to vary freely. The highest value of χ^2 is seen to come for $\Delta m^2_{31} = 0.004$ eV^2 explaining the least allowed area at this value. The figure also illustrates the occurrence of a disallowed window in Δm^2_{31} around $\tan^2\theta_{13} \sim 0.03$, as discussed earlier. Since the solar probabilities are independent of Δm^2_{31} it is clear that the CHOOZ data are responsible for this feature. We have plotted these figures taking the interference term in the CHOOZ probability into account. However, we have explicitly checked that the interfernce term in the CHOOZ probability does not have any impact on the allowed area in the $\Delta m^2_{21} - \tan^2\theta_{12}$ plane. There are two reasons for this. The interference term comes multiplied with s^2_{13} which is confined to very small values. Also the contours that we have plotted are for values of $\Delta m^2_{31} > 1.5 \times 10^{-3}$ eV^2 as allowed by the combined atmospheric and CHOOZ analysis. As is seen from Fig. 1 in this region the interference term does not have any significant effect.

V. SUMMARY, CONCLUSIONS AND DISCUSSIONS

We have performed a three-generation analysis of the solar neutrino and CHOOZ data including the recent SNO CC results. The mass spectrum considered is one where

$\Delta m^2_{21}=\Delta m^2_{\odot}$ and $\Delta m^2_{31}\approx\Delta m^2_{32}=\Delta m^2_{atm}=\Delta_{CHOOZ}$. The other parameters are the three mixing angles θ_{13}, θ_{12} and θ_{23}. For the combined solar and CHOOZ analysis the probabilities are independent of θ_{23}. The solar neutrino probabilities depend on Δm^2_{21}, θ_{12} and θ_{13}. The CHOOZ probability depends mainly on Δm^2_{31} and θ_{13} whereas for $\Delta m^2_{21} \gtrsim 3\times10^{-4}$ eV^2 it depends also on Δm^2_{21} and θ_{12}. The most stringent constraint on the parameter Δm^2_{31} comes from the atmospheric neutrino data. For this we use the updated values from [22,21]. The combined atmospheric+CHOOZ analysis gives $\tan^2\theta_{13}\lesssim0.075$ [21,22]. We keep Δm^2_{31} in the range allowed by the atmospheric neutrino data and determine the allowed values of θ_{13} from a combined analysis of solar and CHOOZ data. The inclusion of the SNO results puts a more restrictive bound on $\theta_{13}-\tan^2\theta_{13}<0.065$. The best fit comes in the LMA region of the $\Delta m^2_{21}-\tan^2\theta_{12}$ plane with $\tan^2\theta_{13}=0.0$, i.e., at the two generation limit. We present the allowed region in the $\Delta m^2_{21}-\tan^2\theta_{12}$ parameter space for various values of $\tan^2\theta_{13}$ and Δm^2_{31} belonging to their respective allowed ranges and determine the changes in the two-generation allowed region due to the presence of the mixing with the third generation. Since very low values of θ_{13} are allowed from combined solar and CHOOZ analysis there is not much change in the two generation allowed regions. No allowed area is obtained in the SMA region at 3σ if one restricts $\tan^2\theta_{13}$ to be <0.065, as allowed by combined solar and CHOOZ analysis.

The combination of solar, atmospheric and CHOOZ data allows one to fix the elements of the neutrino mixing matrix. The U_{e3} element is narrowed down to a small range $\lesssim0.255$ from the solar+CHOOZ analysis including SNO. The θ_{23} mixing angle is $\approx\pi/4$ from atmospheric data [22,21]. This determines the mixing matrix elements $U_{\mu3}$ and $U_{\tau3}$. The θ_{12} mixing angle is limited by the solar data and the tilt is towards large $\tan^2\theta_{12}$. The mixing matrix at the best-fit value of solar+CHOOZ analysis is

$$U\simeq\begin{pmatrix} 2\sqrt{\frac{2}{11}} & \sqrt{\frac{3}{11}} & 0 \\ -\sqrt{\frac{3}{22}} & \frac{2}{\sqrt{11}} & \frac{1}{\sqrt{2}} \\ \sqrt{\frac{3}{22}} & -\frac{2}{\sqrt{11}} & \frac{1}{\sqrt{2}} \end{pmatrix}. \tag{19}$$

Thus the best-fit mixing matrix is one where the neutrino pair with larger mass splitting is maximally mixed whereas the pair with splitting in the solar neutrino range has large *but not* maximal mixing. It is a challenging task from the point of view of model building to construct such scenarios.[3]

From the perspective of model building an attractive possibility is one where both pairs are maximally mixed [35]. Our two generation analysis of the solar data showed that for the LMA MSW region maximal mixing is not allowed at 99.73% C.L. though it is allowed for the LOW [10,12] solution.[4] However, Fig. 4 of this paper shows that three generation analysis allows $\tan^2\theta_{12}=1.0$ with Δm^2_{21} in the LMA region at 99.73% C.L. for Δm^2_{31} in its lower allowed range $\sim1.5\times10^{-3}$ eV^2 and for $\tan^2\theta_{13}\sim0.02$. As Δm^2_{31} increases $\theta_{12}=\pi/4$ in the LMA region no longer remains allowed even at 99.73% level though it remains allowed in the LOW-QVO region. Further narrowing down of the $\Delta m^2_{12}-\tan^2\theta_{12}$ parameter space is expected to come from experiments like KamLand and Borexino which will be able to distinguish between the LMA and LOW regions.

Note added. After submission of our manuscript a paper [36] appeared which finds constraints on $|U_{e3}|^2$ from a similar three generation analysis of the CHOOZ data.

ACKNOWLEDGMENTS

S.G. wishes to acknowledge the kind hospitality extended to her by the theory group of Physical Research Laboratory.

[3]For a recent study see [34].

[4]See however [14].

[1] SNO Collaboration, Q.R. Ahmad *et al.*, Phys. Rev. Lett. **87**, 071301 (2001).

[2] Super-Kamiokande Collaboration, Y. Fukuda *et al.*, Phys. Rev. Lett. **81**, 1158 (1998); **81**, 4279 (1998).

[3] B.T. Cleveland *et al.*, Astrophys. J. **496**, 505 (1998).

[4] The Kamiokande Collaboration, Y. Fukuda *et al.*, Phys. Rev. Lett. **77**, 1683 (1996).

[5] The SAGE Collaboration, J.N. Abdurashitov *et al.*, Phys. Rev. Lett. **77**, 4708 (1996); Phys. Rev. C **60**, 055801 (1999); The Gallex collaboration, W. Hampel *et al.*, Phys. Lett. B **388**, 384 (1996); **447**, 127 (1999); Gallex collaboration, T. Kirsten, in Neutrino 2 1998, Takayanca, Japan [Nucl. Phys. B (Proc. Suppl.) **77**, 26 (2000)]; The GNO collaboration, M. Altmann *et al.*, Phys. Lett. B **492**, 16 (2000); GNO Collaboration, E. Belloti, in Neutrino 2000, Proceeding of the Conference, Sudbury, Canada [Nucl. Phys. B (Proc. Suppl.) **91**, 44 (2001)].

[6] V. Barger, D. Marfatia, and K. Whisnant, Phys. Rev. Lett. **88**, 011302 (2002).

[7] G.L. Fogli, E. Lisi, D. Montanino, and A. Palazzo, Phys. Rev. D **64**, 093007 (2002).

[8] C. Giunti, Phys. Rev. D **65**, 033006 (2002).

[9] J.N. Bahcall, M.C. Gonzalez-Garcia, and C. Pana-Garay, J. High Energy Phys. **08**, 014 (2001).

[10] A. Bandyopadhyay, S. Choubey, S. Goswami, and K. Kar, Phys. Lett. B **519**, 83 (2001).

[11] P. Creminelli, G. Signorelli, and A. Strumia, J. High Energy Phys. **05**, 052 (2001).

[12] S. Choubey, S. Goswami, K. Kar, H.M. Antia, and S.M. Chitre, Phys. Rev. D **64**, 113001 (2001).

[13] P.I. Krastev and A.Yu. Smirnov, Phys. Rev. D **65**, 073022 (2002).

[14] S. Choubey, S. Goswami, and D.P. Roy, Phys. Rev. D **65**, 073001 (2002).
[15] M.V. Garzelli and C. Giunti, J. High Energy Phys. **12**, 017 (2001).
[16] The Super-Kamiokande Collaboration, Y. Fukuda *et al.*, Phys. Lett. B **433**, 9 (1998); **436**, 33 (1998); Phys. Rev. Lett. **81**, 1562 (1998); The Super-Kamiokande Collaboration, S. Fukuda *et al.*, *ibid.* **85**, 3999 (2000).
[17] C. Athanassopoulos *et al.*, Phys. Rev. Lett. **75**, 2650 (1995); C. Athanassopoulos *et al.*, *ibid.* **81**, 1774 (1998); Talk presented by the LSND Collaboration, in Neutrino 2000, Sudbury, Canada, 2000.
[18] J.J. Gomez-Cadenas and M.C. Gonzalez-Garcia, Z. Phys. C **71**, 443 (1996); N. Okada and O. Yasuda, Int. J. Mod. Phys. A **12**, 3669 (1997); S. Goswami, Phys. Rev. D **55**, 2931 (1997); S.M. Bilenky, C. Giunti, and W. Grimus, *ibid.* **57**, 1920 (1998); **58**, 033001 (1998); V. Barger, S. Pakvasa, T.J. Weiler, and K. Whisnant, *ibid.* **58**, 093016 (1998).
[19] M.C. Gonzalez-Garcia, M. Maltoni, and C. Pena-Garay, hep-ph/0108073, and references therein; K.S. Babu and R.N. Mohapatra, Phys. Lett. B **522**, 287 (2001); S. Goswami and A. Joshipura, Phys. Rev. D **65**, 073025 (2002).
[20] M. Appolonio *et al.*, Phys. Lett. B **466**, 415 (1999); **420**, 397 (1998).
[21] G.L. Fogli, E. Lisi, A. Montamino, and A. Palazzo, hep-ph/0104221.
[22] M.C. Gonzalez-Garcia, M. Maltoni, C. Pena-Garay, and J.W.F. Valle, Phys. Rev. D **63**, 033005 (2001).
[23] R. Barbieri *et al.*, J. High Energy Phys. **12**, 017 (1998); V. Barger and K. Whisnant, Phys. Rev. D **59**, 093007 (1999).
[24] We have generalized the approach given in G.L. Fogli, E. Lisi, D. Montanino, and A. Palazzo, Phys. Rev. D **62**, 113004 (2000) for three flavors.
[25] S.T. Petcov, Phys. Lett. B **434**, 321 (1998); M. Narayan, G. Rajasekharan, and R. Sinha, Mod. Phys. Lett. A **13**, 1915 (1998).
[26] S.T. Petcov, Phys. Lett. B **214**, 139 (1988); **406**, 355 (1997); S.T. Petcov and J. Rich *ibid.* **214**, 137 (1989).
[27] S.T. Petcov, Phys. Lett. B **200**, 373 (1988).
[28] S.T. Petcov and M. Piai, hep-ph/0112074.
[29] J.N. Bahcall, S. Basu, and M.P. Pinsonneault, Astrophys. J. **555**, 990 (2001).
[30] G.L. Fogli and E. Lisi, Astropart. Phys. **3**, 185 (1995).
[31] M.C. Gonzalez-Garcia, P.C. de Holanda, C. Peña-Garay, and J.W.F. Valle, Nucl. Phys. **B573**, 3 (2000).
[32] S. Goswami, D. Majumdar, A. Raychaudhuri, Phys. Rev. D **63**, 013003 (2001); hep-ph/9909453; A. Bandyopadhyay, S. Choubey, and S. Goswami, Phys. Rev. D **63**, 113019 (2001); S. Choubey, S. Goswami, N. Gupta, and D.P. Roy, *ibid.* **64**, 053002 (2001).
[33] R. Foot, R.R. Volkas, and O. Yasuda, Phys. Rev. D **58**, 013006 (1998); S. Choubey, S. Goswami, and K. Kar, Astropart. Phys. **17**, 51 (2002).
[34] W. Grimus and L. Lavoura, Acta Phys. Pol. B **32**, 3719 (2001).
[35] See, for example, V. Barger *et al.*, Phys. Lett. B **437**, 107 (1998).
[36] S.M. Bilenky, D. Nicclo, and S.T. Petcov, hep-ph/0112216.